

EVALUATION OF TIDAL EFFECT ON WATER CONSTITUENT VARIATIONS USING OPTICAL OBSERVATIONS AND TIDE GAUGE RECORDS IN THE DUTCH WADDEN SEA

Behnaz Arabi¹, Mhd. Suhyb Salama¹, and Wouter Verhoef¹

(1) Faculty of Geo-Information Science and Earth Observation, University of Twente, Enschede, Netherlands.

ABSTRACT

In this study, the effect of tide on the variation of concentrations of Chlorophyll-a (Chla) and Suspended Particulate Matters (SPM), retrieved from a complete dataset of diurnal close-range hyperspectral observations recorded at the NIOZ jetty station (NJS) located at the Marsdiep inlet in the Dutch part of the Wadden Sea, was evaluated. The two-stream radiative transfer model 2SeaColor was inverted to retrieve Chla and SPM concentrations per each hyperspectral observation of the quality-controlled dataset. Concurrently with these diurnal observations, tidal information was obtained from the Den Helder station located at 3.7 km from the NJS. From the performed analysis and evaluation of this study, we concluded that the tide has little observable effects on the diurnal changes of SPM concentration at the NJS located in the Dutch part of the Wadden Sea. The results of this evaluation and the favorable location of the NJS, which is not influenced by the tidal phase, will contribute to a better understanding of the seasonal variability of the retrieved Chla and SPM concentration values using diurnal optical observations at the NJS. These long-term retrievals can be used later to do the phenological analysis of Chla concentration values in this region.

Index Terms— Radiative transfer modeling (RTM), 2SeaColor model, hyperspectral observations, tidal effect, the NIOZ jetty station.

1. INTRODUCTION

It is important to understand the effect of tides and its related physical processes on water quality and coastal water studies [1]. Since using traditional in-situ measurements of Chla and SPM is very expensive and time-consuming, close-range remote sensing observations with a high temporal resolution were utilized to analyze the tide effects on the related water constituent variations retrieved from watercolor measurements [2]. In this study, for the first time, the effect of the tidal cycle during ebb and flood was

evaluated to detect its influence on the retrieved Chla and SPM concentrations from daily close-range hyperspectral observations at the NJS.

2. STUDY AREA

The SPOT image in the upper-left panel of Figure 1 shows the location of the NJS (marked as a red dot) in the southern part of the Wadden Sea nearby the Marsdiep inlet (53°00'06"N; 4°47'21"E). This inlet is bordered by the island Texel to the north and the town of Den Helder to the south on the mainland [3].

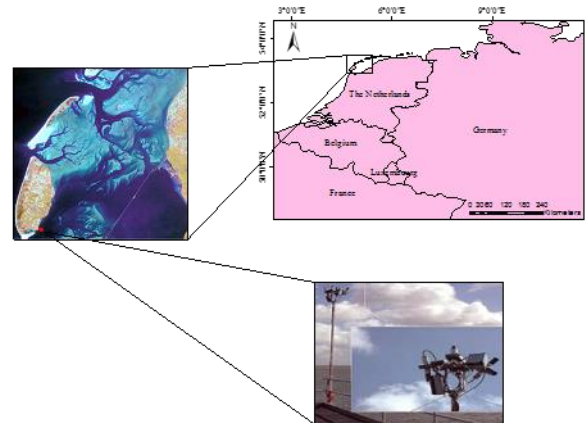


Figure 1. Upper-right: the Southwestern part of the Dutch Wadden Sea in Europe; Upper-left: one SPOT satellite image covering the Dutch Wadden Sea and parts of IJsselmeer lake (8th of May 2006); Bottom: the optical sensors installed on the NIOZ jetty station [4].

The bottom-left panel also shows the autonomous optical sensors installed at the NJS operating from 2002 until present.

3. DATASET

3.1. Close-range hyperspectral observations:

The first dataset contains every fifteen minutes of close-range hyperspectral observations which are being collected using the newest generation of TRIOS Ramses hyperspectral radiometers in order to “autonomous” monitoring of the Dutch Wadden Sea by the Royal Netherlands Institute for Sea Research (the NJS) on the Texel Island from 04:00 to 21:00 UTC since 2001 until present. For more detailed information on the measurement setup of the NJS, the readers are referred to [5].

3.2. Tidal information dataset:

The tidal information dataset contains the measurements of high and low water depth level during the ebb and flood events between 2007 and 2010. The diurnal information was collected from the Den Helder station (52.9667° N, 4.7500° E) located at roughly 3.7 km far from the NJS.

4. METHODOLOGY

4.1. Data quality control:

We implemented the method of Wernand (2002) [5] to perform data quality control on the measurements. This method detects unreliable observations due to three main problems: (i) weather conditions, (ii) spectral shape and (iii) sun glint contamination. In addition, as the results of previous studies show [4], the accuracy of the retrieved water constituent concentrations from watercolor observations deteriorate significantly in parallel with the Solar Zenith Angle (SZA) [4]. Therefore, an SZA flagging by [4] was used for the removal of those measurements, which were collected under the condition of $SZA > 60^\circ$.

4.2. The 2SeaColor model:

The 2SeaColor model is based on the solution of the two-stream radiative transfer equations including direct sunlight, as described by [6,7]. Both the analytical forward model and the inversion scheme are provided in detail in [8]. The reflectance result predicted by the 2SeaColor model is r_{sd}^∞ , the directional-hemispherical reflectance (DHRF) of the semi-infinite medium, which is linked to IOPs by [8]:

$$r_{sd}^\infty = \frac{\sqrt{1+2x} - 1}{\sqrt{1+2x} + 2\mu_w} \quad (1)$$

where x is the ratio of backscattering to absorption coefficients ($x = b_b/a$), and μ_w is the cosine of the solar zenith angle beneath the water surface. The reflectance factor r_{sd}^∞ can be approximated by $Q \times R(0^-)$ under sunny conditions, where $Q = 3.25$ and $R(0^-)$ is the irradiance reflectance beneath the surface [9], which can be converted to above-surface remote sensing reflectance (R_{RS}) by [10].

$$R_{RS} = \frac{0.52 \times R(0^-)}{1 - 1.7 \times R(0^-)} \quad (2)$$

Total absorption and backscattering coefficient of water constituent (a and b_b) were also calculated using the below equations following previous studies of [11,12] respectively.

$$a(\lambda) = a_w(\lambda) + a_{chl}(\lambda) + a_{nap}(\lambda) + a_{cdom}(\lambda) \quad (3)$$

$$b_b(\lambda) = b_{bw}(\lambda) + b_{b,chl}(\lambda) + b_{b,nap}(\lambda) \quad (4)$$

To compute a and b_b values, different parameterization models which have shown reliable results for our case were used from previous studies [4,12]. In this study, we inverted the 2SeaColor model (Equation. 1) to retrieve the concentration values of Chla [mg m^{-3}] and SPM [g m^{-3}] from the close-range hyperspectral observations. We used an iterative optimization approach for the model inversion. We used the “Trust Region” algorithm, which is implemented in the MATLAB (The MathWorks, Inc. Natick, MA, USA) function “lsqnonlin”, in order to minimize the cost function. The cost function computed the Root Mean Square Error (RMSE) between the observed and modeled spectral values for the whole wavelength region of all spectra [13,14].

Table 1. The initial guess of parameters used in the model inversion [4].

Parameter	Unit	Lower/Upper boundary	Initial Guess
Chla concentration	mg m^{-3}	0 - 50	0.1
SPM concentration	g m^{-3}	0 - 100	20
CDOM absorption	m^{-1}	0 - 3	0.25

The results of this inversion technique, for both of the water spectra simulations and water constituent concentrations retrievals, were validated against in-situ measurements in previous studies and showed reliable accuracy [4]. For those observations which were at ebb or flood according to data collected at the Den Helder station, the 2SeaColor model was inverted to retrieve Chla and SPM concentration values for each hyperspectral observation of the quality-controlled dataset (flood: 508, ebb: 383) at the NJS. The selected datasets were divided into two flood and ebb categories based on their tide occurrence time. Each ebb and flood category was divided into another four sub-groups based on their SZA values acquired at the time of data collection. ($SZA < 37.5^\circ$, $37.5^\circ \leq SZA < 45^\circ$, $45^\circ \leq SZA < 52.5^\circ$, $52.5^\circ \leq SZA < 60^\circ$). Then the mean values of the retrieved Chla and SPM concentrations for each SZA sub-group were computed separately. The differences of these mean values were later computed in order to evaluate whether the tide causes any significant variation in the water constituent concentrations.

5. RESULTS

Figure 2 shows the visual representation of the tidal effects on the retrieved Chla and SPM concentration values from the hyperspectral observations using the 2SeaColor model.

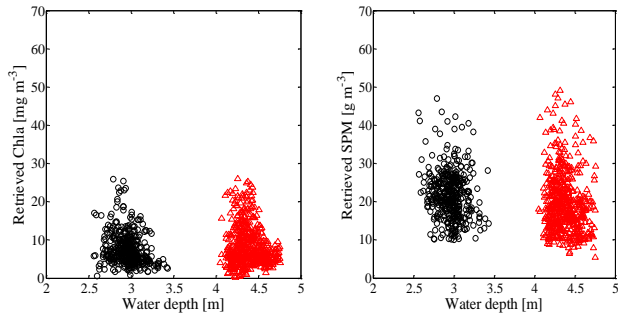


Figure 2. Left: scatter plot of retrieved Chla concentration values [mg m^{-3}] versus water depth [m] at ebb and flood for the quality-controlled dataset at the NJS between 2007 and 2010; Right: same, for retrieved SPM concentration values [g m^{-3}][4].

As can be seen from Figure 2, the retrieved values of Chla and SPM concentrations are plotted against their ebb and flood events (black circle: ebb, red triangle: flood). As this figure shows, the retrieved concentration values of Chla and SPM do not show any significant correlations with the water depth level. The Chla variations are in the same range (between 0 and 30 mg m^{-3}) for both flood and ebb groups. The same is true for the retrieved SPM concentration values with the range of 0 to 50 for the ebb and flood. Table 2 also presents the statistical results of this evaluation.

Table 2. The mean values of retrieved Chla and SPM concentrations for the flood and ebb groups corresponding to their SZA degrees for the quality-controlled dataset between 2007 and 2010 at the NJS [4].

SZA / water constituent	Chla [mg m^{-3}]		SPM [g m^{-3}]	
	flood	ebb	flood	ebb
[$30^\circ - 37.5^\circ$]	7.02	7.10	17.25	19.15
[$37.5^\circ - 45^\circ$]	9.77	8.66	17.66	20.61
[$45^\circ - 52.5^\circ$]	9.93	8.78	20.39	22.86
[$52.5^\circ - 60^\circ$]	8.10	7.93	24.60	26.01

Table 3. The standard deviation values (STDV) between retrieved Chla and SPM concentrations and the flood and ebb groups corresponding to their SZA degrees for the quality-controlled dataset between 2007 and 2010 at the NJS [4].

SZA / water constituent	STDV		STDV	
	flood	ebb	flood	ebb
[$30^\circ - 37.5^\circ$]	0.113	0.09	11.33	0.10
[$37.5^\circ - 45^\circ$]	0.122	0.12	13.45	0.13
[$45^\circ - 52.5^\circ$]	0.156	0.14	16.90	0.15
[$52.5^\circ - 60^\circ$]	14.84	0.20	16.85	0.21

The results of Table 2 shows that there is no large difference between the mean values of retrieved Chla and SPM concentrations under the conditions of flood and ebb for different SZA degrees, since the mean differences are less than 1.15 for Chla [mg m^{-3}] and less than 3 [g m^{-3}] for SPM, in all categories. Only for SPM, we found that the mean values at flood tend to be lower, which might be due to the inflow at the NJS of relatively clear water from the North Sea.

In addition, as the results of Table 3 presents, there is no large difference between the standard deviation values between retrieved Chla concentrations and water depth values as well as retrieved SPM concentrations and water depth values under the conditions of flood and ebb for different SZA degrees. Only these calculated standard deviation values slightly is higher for SPM estimates in comparison to Chla estimates in all categories.

6. CONCLUSIONS

Availability of every fifteen minutes of close-range hyperspectral observations at the NJS, beside the availability of diurnal tidal information from the Den Helder (only 3.7 km far from the NJS), and the fair accuracy of the 2SeaColor model to retrieve the concentrations of Chla and SPM during spring and summer [4,12] gave us this opportunity to evaluate the correlation between the variation of water constituent concentrations and the tidal phase. As the results of this study show, only a negligible relationship was found between diurnal tides and the variation of retrieved SPM values. Thus, it can be said that the NJS is located at a favorable location at the Dutch Wadden Sea, where water constituent concentrations are not significantly influenced by tides. This conclusion helps to investigate the monthly, seasonal and annual variation of WCCs retrieved by the 2SeaColor model from time series of in-situ R_{RS} measurements at the NJS without being concerned about the tidal effect on the variation of these WCC concentrations. Otherwise, the studying of the temporal course becomes very complicated, or in other words, it is fortunate that tidal effects were small, since otherwise we can hardly follow the seasonal courses for further studies.

7. ACKNOWLEDGMENTS

We are very grateful to Dr. Marcel Wernand of NIOZ who provided us with the dataset of water leaving reflectance from hyperspectral observations during this research and helped to explain the measurements at the NIOZ jetty station.

8. REFERENCES

1. Bashir, Z. Modeling the influence of biological activity on fine sediment transport in the Dutch Wadden Sea. Mater thesis. Deltares and University of Twente. **2016**, 1–95.
2. Feng, H.; Campbell, J. W.; Dowell, M. D.; Moore, T. S. Modeling spectral reflectance of optically complex waters using bio-optical measurements from Tokyo Bay. Remote Sensing of Environment. **2005**, 232–243.
3. Hommersom, A. Dense water and Fluid Sand Optical properties and methods for remote sensing of the extremely turbid Wadden Sea. Ph.D Thesis. Vrije Universiteit. Amsterdam. **2010**.
4. Arabi, B.; Salama, M. S.; Wernand, M. R.; Verhoef, W. Retrieval of Suspended Sediment and Chlorophyll-a from Time Series of In-situ Hyperspectral Measurements in the Wadden Sea. Remote Sensing of Environment. Under review. **2017**.

5. Wernand, M. R. Guidelines for (ship-borne) auto-monitoring of coastal and ocean colour. *Ocean Optics*. In; 2002; Vol. 13.
6. Duntley, S. Q. The Optical Properties of Diffusing Materials. *Journal of the Optical Society of America*. **1941**, 61–70.
7. Duntley, S. Q. Light in the Sea. *Journal of the Optical Society of America*. **1963**, 214–233, 53.
8. Salama, M. S.; Verhoef, W. Two-stream remote sensing model for water quality mapping: 2SeaColor. *Remote Sensing of Environment*. **2015**, 111–122, 157.
9. Morel, A.; Gentili, B. Diffuse reflectance of oceanic waters. II Bidirectional aspects. *Applied optics*. **1993**, 6864–6879, 32.
10. Lee, Z.; Carder, K. L.; Arnone, R. A. Deriving inherent optical properties from water color: a multiband quasi-analytical algorithm for optically deep waters. *Applied Optics*. **2002**, 5755–5772, 41.
11. Arnone, R.; Fargion, G.; Wang, M.; Martinolich, P.; Davis, C.; Trees, C.; Ladner, S.; Lawson, A.; Zibordi, G.; Lee, Z.; Ondrusek, M.; Ahmed, S. Ocean Color products from Visible Infrared Imager Radiometer Suite (VIIRS). *International Geoscience and Remote Sensing Symposium (IGARSS)*. **2012**, 287–290.
12. Arabi, B.; Salama, M. S.; Wernand, M. R.; Verhoef, W. MOD2SEA: A Coupled Atmosphere-Hydro-Optical Model for the Retrieval of Chlorophyll-a from Remote Sensing Observations in Complex Turbid Waters. *Remote Sensing*. **2016**.
13. Bayat, B.; van der Tol, C.; Verhoef, W. Remote sensing of grass response to drought stress using spectroscopic techniques and canopy reflectance model inversion. *Remote Sens.* **2016**, 8, 557.
14. Bayat, B.; van der Tol, C.; Verhoef, W. Integrating satellite optical and thermal infrared observations for improving daily ecosystem functioning estimations in a drought episode. *Remote Sens. Environ.* **2018**, 209, 375–394.